Mem. S.A.It. Vol. 83, 230

Memorie della

X-ray pulsars: a review

I. Caballero[1] and J. Wilms[2]

[1] DSM/IRFU/SAp- UMR AIM (7158), CNRS/CEA, University Paris Diderot, 91191 Gif-sur-Yvette, France, e-mail: isabel.caballero@cea.fr
[2] Dr. Karl Remeis Sternwarte & Erlangen Center for Astroparticle Physics, Sternwartstr. 7, 96049 Bamberg, Germany

Abstract. Accreting X-ray pulsars are among the most luminous objects in the X-ray sky. In highly magnetized neutron stars ($B \sim 10^{12}$ G), the flow of matter is dominated by the strong magnetic field. The general properties of accreting X-ray binaries are presented, focusing on the spectral characteristics of the systems. The use of cyclotron lines as a tool to directly measure a neutron star's magnetic field and to test the theory of accretion are discussed. We conclude with the current and future prospects for accreting X-ray binary studies.

Key words. X-rays: binaries - Stars: neutron - Accretion, accretion disks - Magnetic fields

1. Introduction

Accreting X-ray binaries were discovered in the 70's (Giacconi et al. 1971, Tananbaum et al. 1972) and are among the most luminous objects in the X-ray sky. Forty years after their discovery, more than 400 X-ray binaries have been observed, and there is today a deeper knowledge of the physical processes involved in the accretion of matter onto the compact object. In X-ray binaries, matter is accreted from a donor star onto a compact object (white dwarf, neutron star or black hole). X-ray emission originates as a result of the conversion of the gravitational energy of the accreted matter into kinetic energy.

According to the nature of the donor star, X-ray binaries can be classified as High-Mass X-ray Binaries (hereafter HMXBs) or Low-Mass X-Ray Binaries (hereafter LMXBs). Typically, HMXBs have young optical companions of spectral type O or B and mass $M \gtrsim 5M_{\odot}$, and high magnetic fields $B \sim 10^{12}$ G. LMXB systems have older optical companions, with masses in general $M \leq 1\,M_{\odot}$, and lower magnetic fields $B \sim 10^{9-10}$ G. X-ray binaries are numerous objects in the Galaxy, with 114 HMXBs in the Galaxy and 128 HMXBs in the Magellanic Clouds, and 187 LMXBs in the Galaxy and Magellanic Clouds (Liu et al. 2005, 2006, 2007). In accreting neutron stars, due to the inclination of the neutron star's rotational axis with respect to the magnetic axis, the X-ray emission appears pulsated to a distant observer.

In this review, we concentrate on the properties of X-ray binaries with a highly magnetized neutron star ($B \sim 10^{12}$ G). The basic aspects of accreting X-ray pulsars are described, and the current status of the observations and theory of these systems is presented.

Send offprint requests to: I. Caballero, e-mail: isabel.caballero@cea.fr

2. Accretion onto the neutron star

The accretion of matter in X-ray binaries can take place via Roche lobe overflow or via direct wind accretion. Roche Lobe overflow takes place when the donor star evolves, expands and fills its Roche lobe. The matter exceeding the Roche lobe is no longer gravitationally bound to the star and can be accreted by the compact object through the inner Lagrange point. The accreted matter has a large amount of angular momentum, and therefore forms an accretion disk around the compact object instead of being accreted directly. This typically occurs in LMXBs.

Wind accretion takes place in binary systems with a O or B donor star, namely HMXBs. These stars have very strong stellar winds, with a mass loss rate that can be as high as $\dot{M} \sim 10^{-4} - 10^{-6}\,M_\odot/\mathrm{yr}$. The compact object typically orbits the donor star at a distance of less than one stellar radius, and therefore the compact object is deeply embeded in the stellar wind (e.g., Vela X-1, Nagase et al. 1986).

A large fraction of X-ray binaries (about 60% of the HMXBs) falls in the category of Be/X-ray binary systems. These systems have quite eccentric orbits, and their X-ray activity is related to the presence of a disk of material that surrounds the equator of the Be star. They can have giant (type II) or normal (type I) outbursts, and long quiescence periods. See Reig (2011) for a recent review of Be/X-ray binaries.

Independently of the way matter is transferred from the donor star to the compact object, at a distance close to the compact object the flow of matter is dominated by the strong magnetic field of $B \sim 10^{12}\,\mathrm{G}$. The infalling matter follows the magnetic field lines, forming accretion columns on the neutron star magnetic poles. The accreting plasma couples to the magnetic field lines at the Alfvén radius $r_{\mathrm{mag}} = 2.9 \times 10^8 M_1^{1/7} R_6^{-2/7} L_{37}^{-2/7} \mu^{4/7}\mathrm{cm}$, where M_1 is given in units of $1\,M_\odot$, R_6 is given in units of 10^6 cm and L_{37} is the luminosity in units of $10^{37}\,\mathrm{erg\,s^{-1}}$. For typical neutron star parameters, $r_{\mathrm{mag}} \sim 1800\,\mathrm{km}$. Accretion can take place as long as the Alfvén radius is smaller than the co-rotation radius $r_{\mathrm{co}} = \left(\frac{GM}{\omega^2}\right)^{1/3}$ (defined as the radius at which the angular velocity of the magnetosphere ωr and the Keplerian velocity of the disk $\sqrt{GM/r}$ are equal). If this is not the case, the propeller effect can inhibit the accretion (Illarionov & Sunyaev 1975). Such an effect could for instance explain the off-states observed in Vela X-1 (Kreykenbohm et al. 2008).

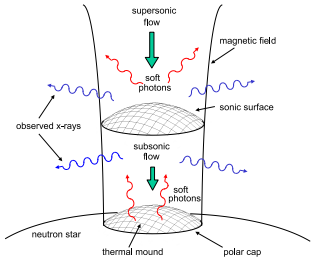

Fig. 1. Schematic view of the accretion column. Seed photons are created along the column via bremstrahlung and cyclotron emission, together with black body seed photons emitted from the surface of the thermal mound. (Figure 1 from Becker & Wolff (2007), reproduced by permission of the AAS.

The luminosity produced by an accreting object is given by $L = GM\dot{m}/R$, where M, R are the mass and radius of the compact object, and $\dot{m}$ is the mass accretion rate. As will be further discussed in Sec. 4, there is a limit on the luminosity that an accreting body can have, the Eddington luminosity, obtained by balancing gravitational force and radiation pressure. For a spherically symmetric accretion and a steady flow, the Eddington luminosity is $L_{\mathrm{Edd}} = \frac{4\pi GMm_{\mathrm{p}}c}{\sigma_{\mathrm{T}}} \approx 1.3 \times 10^{38} \frac{M}{M_\odot}\mathrm{erg\,s^{-1}}$.

3. Formation of the spectral continuum

The X-ray spectrum is typically well described by a power law with an exponential cutoff. Numerous authors have made attempts to derive the shape of X-ray pulsar spectra analytically or numerically (e.g., Nagel 1981, Meszaros & Nagel 1985, Burnard et al. 1991,

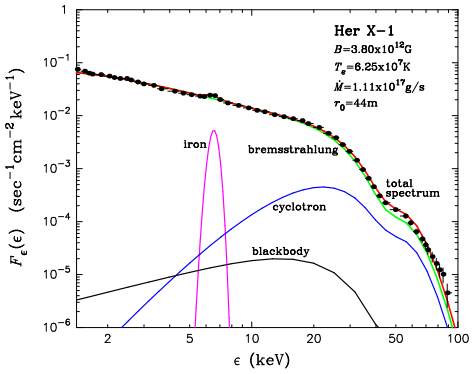

Fig. 2. Theoretical spectrum of Her X-1. The total spectrum (red line) and individual components are shown, together with a BeppoSAX spectrum of the source (black circles). (Figure 6 from Becker & Wolff (2007), reproduced by permission of the AAS).

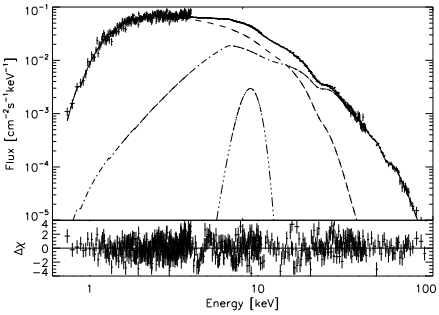

Fig. 3. Unfolded spectrum of 4U 0115+64 and best fit model. The solid line shows the best fit model, sum of the dashed line that represents the thermal Comptonization, the dot-dashed line that shows the column emission, and the dot-dot dashed line that shows a narrow Gaussian line. Lower panel: residuals from the best fit model. From Ferrigno et al. (2009), reproduced with permission © ESO.

Becker & Wolff 2005). However no self-consistent, general model applicable to X-ray sources has been established, due to the complexity of the physical processes that take place in the accretion column and in the magnetosphere. The radiation spectrum or "standard" X-ray continuum (White et al. 1983) is a power law in the $\sim (5-20)$ keV energy range with an exponential cutoff at energies $\sim (20-30)$ keV (Coburn et al. 2002). Additionally, iron fluorescence Fe Kα lines are produced in the circumstellar material, and cyclotron absorption lines also modify the continuum emission (see Sec. 4).

Recently, Becker & Wolff (2007) have developed a model for the continuum formation to reproduce the spectra of bright accreting X-ray pulsars, for which a radiative shock located above the stellar surface dominates the spectral formation. The total observed spectrum is a result of the bulk and thermal Comptonization of bremstrahlung, black body and cyclotron seed photons. A schematic view of the model is shown in Fig. 1. In Fig. 2 a comparison between the theoretical spectrum of Her X-1 and a BeppoSAX observation of the source is shown.

The model is available for spectral fitting in XSPEC (Ferrigno et al. 2009). The authors have applied the model to BeppoSAX observations of the accreting Be/X-ray binary 4U 0115+64 during an outburst. From this study, Ferrigno et al. found that the emission above ~7 keV could be due to thermal and bulk Comptonization of the seed photons produced by cyclotron cooling of the accretion column, plus emission at lower energies due to thermal Comptonization of a blackbody component from a diffuse halo close to the neutron star surface. The data, best fit model, and residuals are shown in Fig. 3.

4. Cyclotron resonance scattering features

The energy of the electrons in the highly magnetized plasma is quantized into Landau levels. Due to the resonant scattering of photons off electrons, absorption-like features can be formed in the X-ray spectrum of X-ray pulsars (cyclotron resonance scattering features or simply cyclotron lines). The energy spacing between the Landau levels is given by

$$E_{\rm cyc} = \hbar \frac{eB}{m_{\rm e}c} = 11.6\,{\rm keV} \cdot B_{12} \qquad (1)$$

where B_{12} is the magnetic field in units of 10^{12} G. Therefore, the measurement of a cyclotron

Table 1. List of sources with cyclotron line(s) significantly detected in their spectrum, updated from Makishima et al. (1999) and Heindl et al. (2004). The cyclotron line energy, the discovery instrument and reference are given. For the last five sources listed there is weak evidence for a cyclotron line but this has not been firmly confirmed.

Source	$E_{\mathrm{n,cyc}}$ (keV)	Discovery	Reference
Swift J1626.6-5156	10	RXTE	DeCesar et al. (2009)
4U 0115+64	14,24,36,48,62	HEAO-1	Wheaton et al. (1979)
4U 1907+09	18,38	Ginga	Makishima & Mihara (1992)
4U 1538-52	20	Ginga	Clark et al. (1990)
Vela X-1	24,52	HEXE	Kendziorra et al. (1992)
V 0332+53	26,49,74	Ginga	Makishima et al. (1990)
Cep X-4	28	Ginga	Mihara et al. (1991)
Cen X-3	28.5	RXTE	Heindl & Chakrabarty (1999)
		BeppoSAX	Santangelo et al. (1998)
X Per	29	RXTE	Coburn et al. (2001)
MXB 0656-072	36	RXTE	Heindl et al. (2003)
XTE J1646+274	36	RXTE	Heindl et al. (2001)
4U 1626-67	37	RXTE	Heindl & Chakrabarty (1999)
		BeppoSAX	Orlandini et al. (1998)
GX 301-2	37	Ginga	Makishima & Mihara (1992)
Her X-1	41	Balloon	Trümper et al. (1977)
A 0535+26	46,100	HEXE	Kendziorra et al. (1992)
1A 1118-61	55	RXTE	Doroshenko et al. (2010)
EXO 2030+375	11?	RXTE	Wilson et al. (2008)
	63?	INTEGRAL	Klochkov et al. (2008a)
GS 1843+00	20?	Ginga	Mihara (1995)
OAO 1657-415	36?	BeppoSAX	Orlandini et al. (1999)
GRO J1008-57	88?	CGRO	Shrader et al. (1999)
LMC X-4	100?	BeppoSAX	La Barbera et al. (2001)

line in the spectrum of a highly magnetized accreting neutron star provides a direct measurement of the neutron star's magnetic field. Due to the strong gravitational field around the neutron star, the cyclotron line energy is gravitationally red-shifted, and the observed line energies have to be corrected as

$$E_n = nE_{\mathrm{cyc}} = (1+z)E_{n,\mathrm{obs}} \quad (2)$$

where the gravitational redshift is $z \sim 1.25 \ldots 1.4$ for typical neutron star parameters.

Since the discovery of a cyclotron line in the X-ray spectrum of Her X-1 in 1976 (Truemper et al. 1978), cyclotron lines have been observed in 16 accreting pulsars (see e.g. Makishima et al. 1999, Heindl et al. 2004, for reviews, and Table 1 for a list of the currently known sources that exhibit cyclotron lines). Several sources exhibit a fundamental line plus harmonics, like V 0332+53 (Kreykenbohm et al. 2005). The record holder is 4U 0115+64, showing up to five cyclotron lines in its spectrum (Santangelo et al. 1999, Heindl et al. 1999).

Cyclotron lines are extremely powerful tools since they provide the *only* direct way to determine the magnetic field of a neutron star, and they can also probe the change of the accretion structure and plasma properties with luminosity.

Matter is channeled onto the magnetic poles by the magnetic field lines creating accretion funnels, where the X-ray emission is originated. As proposed in the pioneering work of Basko & Sunyaev (1976), there are two different accretion regimes according to the mass accretion rate (and hence the luminosity). For luminosities higher than a critical luminosity, which is generally comparable to the Eddington luminosity L_{E} (Nelson et al. 1993),

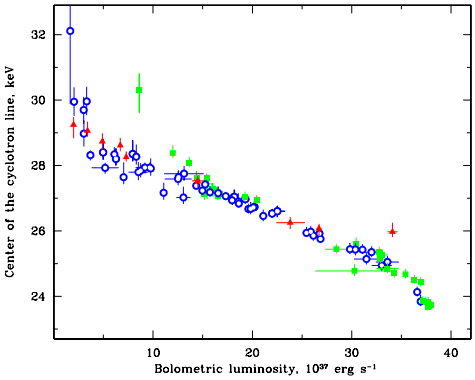

Fig. 4. Evolution of the cyclotron line energy of V 0332+53 with the X-ray luminosity. From Tsygankov et al. (2010), reproduced with the permission from MNRAS.

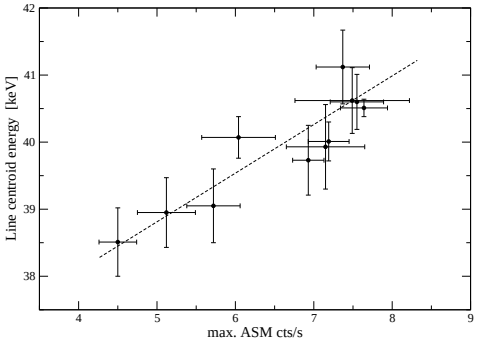

Fig. 5. Dependence of cyclotron line energy with the X-ray luminosity for Her X-1. From Staubert et al. (2007), reproduced with permission © ESO.

a radiation dominated shock is formed in the accretion column. In this case a "fan beam" emission pattern is predicted, in which photons escape perpendicular to the accretion column. For luminosities lower than the critical luminosity, matter can fall almost freely until the neutron star surface, causing the braking of the plasma by a hydrodynamical shock close to the neutron star surface. In this case, X-rays are able to escape vertically along the accretion column, giving rise to a "pencil beam" pattern.

For high luminosity sources it is generally believed that an increase in the mass accretion rate (or increase in luminosity) causes an increase in the height of the accretion column (Burnard et al. 1991, based on Basko & Sunyaev 1976). Assuming a dipole magnetic field, the height of the accretion column can be estimated in terms of the cyclotron energy. Therefore, cyclotron line energy measurements allow us to test this theory. This relation was experimentally confirmed with Ginga observations of 4U 0115+64 (Mihara 1995, Mihara et al. 2004, Nakajima et al. 2006) and RXTE observations of 4U 0115+64 (Nakajima et al. 2006, Tsygankov et al. 2010) and V 0332+53 (Tsygankov et al. 2007). For these sources, a negative correlation between the X-ray luminosity and the cyclotron line energy has been observed (see Fig. 4).

For low luminosity sources in the sub-Eddington regime, a different behavior is expected. Staubert et al. (2007) have discovered for Her X-1 a positive correlation between the cyclotron line energy and the luminosity (see Fig. 5). They find a change in the cyclotron line of 5% for a luminosity variation of $\Delta L/L \sim 1$. In this case, no radiation dominated shock is expected to form in the accretion column. Based on Basko & Sunyaev (1976) and Nelson et al. (1993), where the physics of accretion in low-luminosity sources is studied, Staubert et al. (2007) find the following relation between the cyclotron line energy and the luminosity: $\Delta E_{\rm cyc}/E_{\rm cyc} = 3\frac{l_*}{R}\frac{\Delta L}{L}$ where l_* is the height of the scattering region above the neutron star surface and R is the neutron star radius. For $\Delta L/L \sim 1$, this implies a change of $\sim$3%, very close to the 5% obtained from the Her X-1 observations.

Contrary to the above sources, measurements of the cyclotron line energy of A 0535+26 during a normal outburst in 2005 show no significant correlation between the cyclotron line energy and the luminosity. This suggests that the line forming region does not change with the mass accretion rate of the system (Caballero et al. 2007). A question that is still under debate is whether the transition between the two regimes has been observed.

Changes in the cyclotron line energy have been reported not only with the luminosity, but also with the pulse phase. The cyclotron line

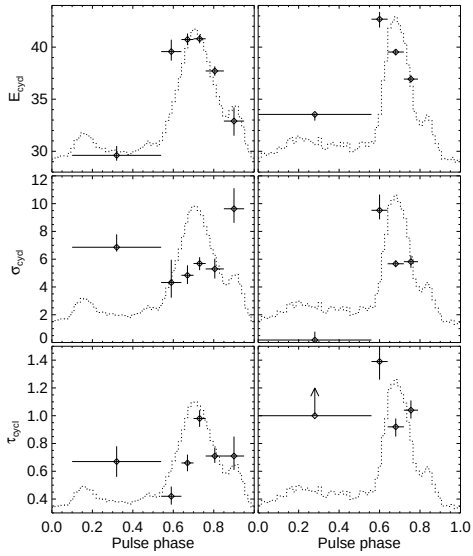

Fig. 6. Variation of the cyclotron line parameters with the pulse phase for Her X-1, during the start of the main-on state (left) and at the end of the main-on state (right). From Klochkov et al. (2008b), reproduced with permission © ESO.

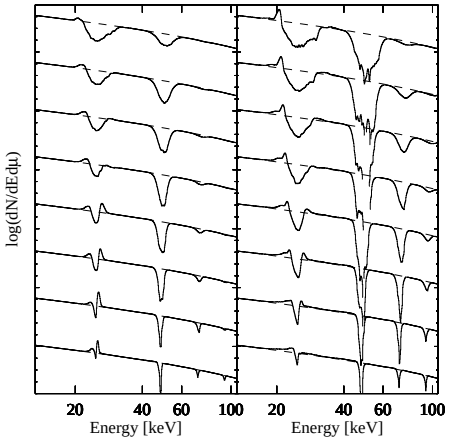

Fig. 7. Simulated cyclotron line shapes for $B/B_{\rm crit} = 0.04$ as a function of angle (decreasing upwards) and optical depth. A cylindrical geometry, a plasma temperature of $kT = 3$ keV, Thomson optical depths of 3×10^4 (left) and 3×10^3 (right) are assumed. Line shapes are rather complex and strongly depend on the physical and geometrical parameters. From Schönherr et al. (2007), reproduced with permission © ESO.

energy values discussed above correspond to phase averaged spectra. However, due to the rotation of the neutron star, during a rotational phase the observer is looking into different regions of the neutron star surface and/or accretion column, and therefore different magnetic fields and continuum parameters can be expected. For GX 301-2, Kreykenbohm et al. (2004) have shown that the cyclotron line energy varies by 25%, implying a variation of the magnetic field between 3.4×10^{12} and 4.2×10^{12} G. For Her X-1, Klochkov et al. (2008b) have also found a variation of the cyclotron line and continuum parameters with the pulse phase (see Fig. 6), that they interpret with different viewing angles of the neutron star along the rotational phase.

Until recently, only phenomenological models (Gaussian or Lorentzian curves) were used to describe the cyclotron lines observed in the spectra of accreting X-ray pulsars. However, Monte Carlo simulations of the propagation of photons through a low density plasma assumed to be threaded by an uniform magnetic field have revealed that the cyclotron lines are expected to vary in shape, depth and width over the pulse (Araya & Harding 1999, Araya-Góchez & Harding 2000, Schönherr et al. 2007, see Fig. 7). A complex line profile has also emerged from observations (e.g., in V 0332+53, Pottschmidt et al. 2005). A Monte Carlo code based on the code of Araya & Harding (1999), Araya-Góchez & Harding (2000) has been implemented in XSPEC by (Schönherr et al. 2007). First fits have been performed to Cen X-3 data (Suchy et al. 2008). The new model allows to narrowly constrain the main physical parameters of the system, as the plasma geometry (slab versus cylinder), the electron parallel temperature, and density. The latest version of the model allows for complex geometries, magnetic field gradients, and velocity gradients (Schwarm 2010).

5. Conclusions

We have reviewed the general properties of accreting X-ray pulsars, in particular the spectral formation and cyclotron lines. Many aspects of accreting X-ray pulsars have not been discussed in this review, like pulse profile formation. Modeling of pulse profiles has been performed for instance by Wang & Welter (1981), Meszaros & Nagel (1985), and Leahy (1991). An alternative pulse profile decomposition method has been proposed by Kraus et al. (1995), that allows to infer geometrical parameters of the neutron star, and to reconstruct the emission beam pattern that can be compared to model predictions (see Kraus et al. (2003) and e.g. Sasaki et al. 2010). Also not discussed in this review are the relativistically broadened lines that have been observed in several neutron star X-ray binaries. These can be used to constrain neutron star parameters and the equation of state, see, e.g., Cackett et al. (2008) but also Done & Diaz Trigo (2010).

Forty years after the discovery of the first accreting neutron star, the continuum formation is now better understood, but still many questions are open. There are now 16 neutron stars with direct magnetic field determinations – now enough data available for both, individual studies, and study as a class. The cyclotron line behavior with the X-ray luminosity allows deeper probing of accretion column theory. Good numerical models for cyclotron line formation are available, and the behavior of the lines is roughly in agreement with predictions of Monte Carlo computations.

In the future, MAXI (Matsuoka et al. 2009) and Swift/BAT (Barthelmy et al. 2005) will continue to monitor the X-ray sky and discover neutron star outbursts. ASTROSAT (O'Brien 2011) will allow routine measurements of broadband spectral shape and magnetic fields, NuStar (Harrison et al. 2005) will start to resolve the shape of cyclotron lines, while LOFT (Feroci et al. 2010) and Athena will allow studies at characteristic variability timescale. With the current and future missions, we have reached a very exciting era in which high quality data are available together with physical models that will allow a deeper understanding of the extreme physics involved in the accretion of matter onto a neutron star.

Acknowledgements. IC acknowledges financial support from the French Space Agency CNES through CNRS, and Andrea Santangelo for the help in the organization and the strong support. The authors acknowledge Franco Giovannelli and organizers for the invitation to the conference, and thank the MAGNET collaboration and Katja Pottschmidt for her useful comments on the manuscript. JW acknowledges partial support by DLR grant 50 OR 1007.

References

Araya, R. A. & Harding, A. K. 1999, ApJ, 517, 334
Araya-Góchez, R. A. & Harding, A. K. 2000, ApJ, 544, 1067
Barthelmy, S. D., et al. 2005, Space Science Reviews, 120, 143
Basko, M. M. & Sunyaev, R. A. 1976, MNRAS, 175, 395
Becker, P. A. & Wolff, M. T. 2005, ApJ, 630, 465
Becker, P. A. & Wolff, M. T. 2007, ApJ, 654, 435
Burnard, D. J., Arons, J., & Klein, R. I. 1991, ApJ, 367, 575
Caballero, I., et al. 2007, A&A, 465, L21
Cackett, E. M., et al. 2008, ApJ, 674, 415
Clark, G. W., et al. 1990, ApJ, 353, 274
Coburn, W., et al. 2001, ApJ, 552, 738
Coburn, W., et al. 2002, ApJ, 580, 394
DeCesar, M. E., Boyd, P. T., Markwardt, C. B., et al. 2009, in BAAS, Vol. 41, AAS Meeting Abstracts 213, 432.02
Done, C. & Diaz Trigo, M. 2010, MNRAS, 407, 2287
Doroshenko, V., et al. 2010, A&A, 515, L1
Feroci, M., et al. 2010, in Proc. SPIE, Vol. 7732
Ferrigno, C., Becker, P. A., Segreto, A., Mineo, T., & Santangelo, A. 2009, A&A, 498, 825
Giacconi, R., et al. 1971, ApJ, 167, L67
Harrison, F. A., et al. 2005, Experimental Astronomy, 20, 131
Heindl, W., Coburn, W., Kreykenbohm, I., & Wilms, J. 2003, ATEL, 200

Heindl, W. A. & Chakrabarty, D. 1999, in Highlights in X-ray Astronomy, ed. B. Aschenbach & M. J. Freyberg, 25
Heindl, W. A., et al. 1999, ApJ, 521, L49
Heindl, W. A., et al. 2001, ApJ, 563, L35
Heindl, W. A., et al. 2004, in American Institute of Physics Conference Series, Vol. 714, X-ray Timing 2003: Rossi and Beyond, ed. P. Kaaret, F. K. Lamb, & J. H. Swank, 323–330
Illarionov, A. F. & Sunyaev, R. A. 1975, A&A, 39, 185
Kendziorra, E., et al. 1992, in The Compton Observatory Science Workshop, ed. C. R. Shrader, N. Gehrels, & B. Dennis, 217
Klochkov, D., Santangelo, A., Staubert, R., & Ferrigno, C. 2008a, A&A, 491, 833
Klochkov, D., et al. 2008b, A&A, 482, 907
Kraus, U., Nollert, H.-P., Ruder, H., & Riffert, H. 1995, ApJ, 450, 763
Kraus, U., Zahn, C., Weth, C., & Ruder, H. 2003, ApJ, 590, 424
Kreykenbohm, I., et al. 2005, A&A, 433, L45
Kreykenbohm, et al. 2004, A&A, 427, 975
Kreykenbohm, et al. 2008, A&A, 492, 511
La Barbera, A., Burderi, L., Di Salvo, T., Iaria, R., & Robba, N. R. 2001, ApJ, 553, 375
Leahy, D. A. 1991, MNRAS, 251, 203
Liu, Q. Z., van Paradijs, J., & van den Heuvel, E. P. J. 2005, A&A, 442, 1135
Liu, Q. Z., van Paradijs, J., & van den Heuvel, E. P. J. 2006, A&A, 455, 1165
Liu, Q. Z., van Paradijs, J., & van den Heuvel, E. P. J. 2007, A&A, 469, 807
Makishima, K. & Mihara, T. 1992, in Frontiers Science Series, ed. Y. Tanaka & K. Koyama, 23
Makishima, K., et al. 1990, ApJ, 365, L59
Makishima, K., Mihara, T., Nagase, F., & Tanaka, Y. 1999, ApJ, 525, 978
Matsuoka, M., et al. 2009, PASJ, 61, 999
Meszaros, P. & Nagel, W. 1985, ApJ, 299, 138
Mihara, T. 1995, PhD thesis, Dept. of Physics, Univ. of Tokyo
Mihara, T., et al. 1991, ApJ, 379, L61
Mihara, T., Makishima, K., & Nagase, F. 2004, ApJ, 610, 390
Nagase, F., et al. 1986, PASJ, 38, 547
Nagel, W. 1981, ApJ, 251, 288
Nakajima, M., Mihara, T., Makishima, K., & Niko, H. 2006, ApJ, 646, 1125
Nelson, R. W., Salpeter, E. E., & Wasserman, I. 1993, ApJ, 418, 874
O'Brien, P. 2011, Advances in Space Research, 47, 1451
Orlandini, M., et al. 1999, A&A, 349, L9
Orlandini, M., et al. 1998, in The Active X-ray Sky: Results from BeppoSAX and RXTE, ed. L. Scarsi, H. Bradt, P. Giommi, & F. Fiore, 158
Pottschmidt, K., et al. 2005, ApJ, 634, L97
Reig, P. 2011, Ap&SS, 332, 1
Santangelo, A., et al. 1998, A&A, 340, L55
Santangelo, A., et al. 1999, ApJ, 523, L85
Sasaki, M., et al. 2010, A&A, 517, A8
Schönherr, G., et al. 2007, A&A, 472, 353
Schwarm, F. 2010, diploma Thesis, Dr. Karl Remeis Observatory Bamberg, University of Erlangen-Nrnberg
Shrader, C. R., Sutaria, F. K., Singh, K. P., & Macomb, D. J. 1999, ApJ, 512, 920
Staubert, R., et al. 2007, A&A, 465, L25
Suchy, S., et al. 2008, ApJ, 675, 1487
Tananbaum, H., et al. 1972, ApJ, 174, L143
Truemper, J., et al. 1978, ApJ, 219, L105
Trümper, J., Pietsch, W., Reppin, C., & Sacco, B. 1977, in New York Academy Sciences Annals, Vol. 302, Eighth Texas Symposium on Relativistic Astrophysics, ed. M. D. Papagiannis, 538
Tsygankov, S. S., Lutovinov, A. A., Churazov, E. M., & Sunyaev, R. A. 2007, Astronomy Letters, 33, 368
Tsygankov, S. S., Lutovinov, A. A., & Serber, A. V. 2010, MNRAS, 401, 1628
Wang, Y.-M. & Welter, G. L. 1981, A&A, 102, 97
Wheaton, W. A., et al. 1979, Nature, 282, 240
White, N. E., Swank, J. H., & Holt, S. S. 1983, ApJ, 270, 711
Wilson, C. A., Finger, M. H., & Camero-Arranz, A. 2008, ApJ, 678, 1263